# On the coupling of COSMO to WAM

**Luigi Cavaleri[1], Aron Roland[2], Mathieu Dutour[3], Luciana Bertotti[1], and Lucio Torrisi[4]**

*[1] Institute of Marine Sciences, ISMAR-CNR, Venice, Italy*
*[2] Institute for Hydraulic and Water Resources Engineering, Tech. Univ. Darmstadt, Germany*
*[3] Institute Ruder Boskovic, Zagreb, Croatia*
*[4] Italian Meteorological Service, CNMCA, Rome, Italy*

**Abstract**

We describe the two-way coupling between the COSMO limited area meteorological and the WAM wave models. Following the approach first used at the European Centre for Medium-Range Weather Forecasts at the global scale, the coupling is achieved by passing from COSMO to WAM the air density and the 10 m height wind, while in the other direction the flowing info concerns the Charnock coefficient representative of the wave induced surface roughness. The coupling does not affect the original turbulence closure of the COSMO meteorological model.

The different decomposition used in the two models, simple for COSMO, more complicated, but computer effective, in the case of WAM, implies special care in the interpolation, especially at the interface between land and sea. COSMO has been kept as the leading model.

Still in the development stage, the coupled model system has been applied with 0.25 degree resolution for a two month period, Nov-Dec 2010. The area of interest is the Mediterranean Sea. The results, obtained without data assimilation, but simply driven by the boundary conditions, show the expected reduction of the wind speed and wave height in areas of active generation, together with a more limited deepening of the developing cyclones. The reduction is particularly evident in areas characterised by strong wind and short fetch, typically bora and mistral, where the air-sea interaction processes are extremely active.

## 1. Introduction

The coupling of waves to the atmosphere is an obvious and necessary step toward a unified approach in order to improve the description of the atmospheric boundary layer and the forecast of ocean waves. This approach was already shown by Janssen et al. (2004) to improve both atmosphere and surface wave forecast on global scale. In the same work it was also emphasized that with increasing resolution in geographical space, the influence of the coupling of both systems has an increasing impact on the results for both the surface waves and the atmosphere. Following these facts it is a logical step to couple local weather prediction models, such as COSMO (German Weather Service), to a surface modelling system such as WAM (WAMDI group, 1988), to account for these interactions also at local scale.

Our long term plan is to have a fully coupled limited area atmosphere-wave-ocean system. At the present stage of development we have just focused on the exchange of momentum between the atmosphere and the waves and on the apparent roughness length felt by the lowest layers of the atmosphere based on the surface wave model. However, future challenges are defined through the fact

that the ocean waves have a strong influence on the diurnal SST (eg., Janssen, 2011) and of course on the water vapour fluxes, whereas strong winds may lead to the formation of sea spray and introduce in that way the damping of wave growth due the reduction of the apparent roughness length (e.g., Makin, 2005; see also Cavaleri et al., 2012, for a related extensive discussion). Therefore, in the next stage of this project the coupling of the circulation model ROMS will be undertaken and the wave turbulence generation will be considered based on the work of Ardhuin & Jenkins (2006), Babanin et al. (2006) and Janssen (2011)

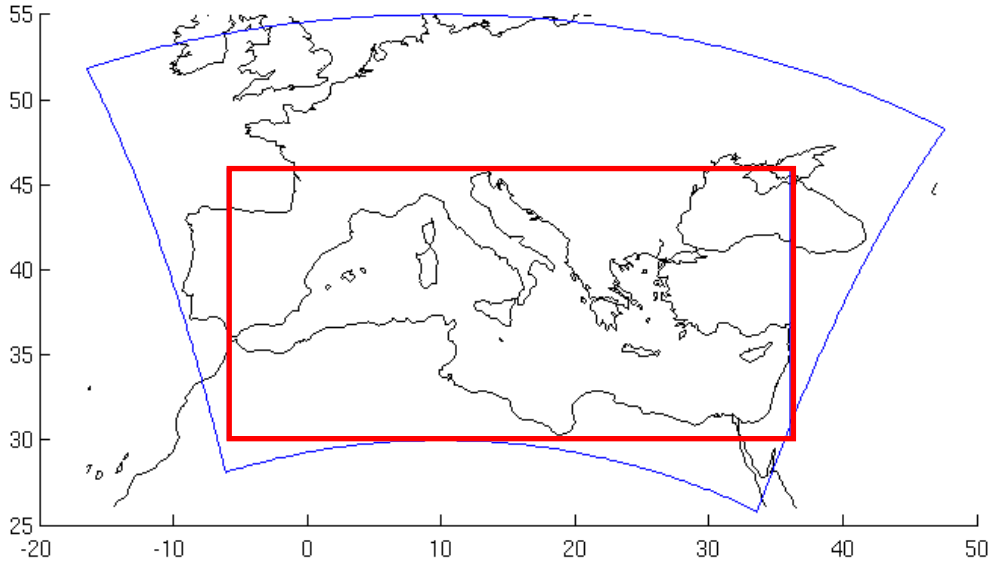


*Figure 1: Domains of the coupled model. The blue line indicates the COSMO domain. The red one indicates the WAM domain for the Mediterranean Sea.*

In this part of the project, focused on the Mediterranean Sea (see Figure 1), we successfully coupled the WAM model to the COSMO model using a novel coupling library, written in native FORTRAN, especially conceived to fit the needs of both the models with respect to the parallel framework prescribed by the implementations. These needs derive from the historical evolution of the WAM code developed at a time when the computer memories were very limited. However, the approach in the WAM model, although complicated, is very effective, and therefore the coupling library was especially designed to fit the way the domain decomposition is done in the WAM model, but keeping in mind that in the future ROMS will be coupled as well. Therefore we have formulated the code so that the decomposition technique used in ROMS can also be easily embedded in the developed coupling library.

The document is organized as follows. In the first part of the manuscript (Section 2) we give a short introduction to the numerical models, followed (Section 3) by a brief description of the physics of the atmospheric boundary layer. We describe the physics of both of the models and of how they approximate the physics at the ocean interface, where this work is focused on. In the third part (Section 4) we give a description of the newly designed coupling library followed in Section 5 by the validation of the model results on the base of extensive comparisons with measured data. The paper

is concluded by a short discussion, Section 6, where we summarise the overall results and hint to future developments.

# 2. Models structure

## 2.1. The WAM model

The global ocean WAve prediction Model called WAM was the first third generation wave model and it was conceived by the WAMDI group (WAMDI, 1988). WAM has as prognostic variable the two-dimensional wave spectrum from which diagnostic variables, such as significant wave height, average wave period and many other integral wave parameters can be deduced. The WAM model is used at the European Centre for Medium-Range Weather Forecasts (ECMWF, Reading, U.K.) as the operational wave model. It is tightly coupled to the local IFS (Integrated Forecasting System, ECMWF, 2012). To have a local modelling environment that conforms with the one at ECMWF, in our work we have followed closely the theoretical basis established there by Peter Janssen (1989, 1991).

In particular the WAM model solves the Wave Action Equation (hereinafter WAE) based on the work of Klaus Hasselman (Hasselmann, 1961). The WAE describes the evolution of random waves in terms of the two-dimensional wave spectrum taking into account the influence of slowly varying media.

$$\underbrace{\frac{\partial}{\partial t}N}_{\text{Change in Time}} + \underbrace{\nabla_{\mathbf{X}}\left(\dot{\boldsymbol{X}}N\right)}_{\text{Advection in horizontal space}} + \underbrace{\frac{\partial}{\partial\sigma}\left(\dot{\theta}N\right)+\frac{\partial}{\partial\theta}\left(\dot{\sigma}N\right)}_{\text{Advection in spectral space}} = \underbrace{S_{tot}}_{\text{Total Source Term}} \qquad \text{eq.1}$$

where the wave action is defined as the conserved quantity in slowly varying environment according to Bretherton and Garrett (1969) as:

$$N_{(t,\mathrm{X},\sigma,\theta)} = \frac{E_{(t,\mathrm{X},\sigma,\theta)}}{\sigma} \qquad \text{eq.2}$$

The advection velocities in the different phase spaces can be defined by the following equations (e.g. Keller, 1958).

$$\dot{\boldsymbol{X}} = \boldsymbol{c}_X = \frac{d\boldsymbol{X}}{dt} = \frac{d\omega}{dk} = \boldsymbol{c_g} + \boldsymbol{U}_A \qquad \text{eq.3a}$$

$$\dot{\theta} = c_\theta = \frac{1}{k}\frac{\partial\sigma}{\partial d}\frac{\partial d}{\partial m} + \boldsymbol{k}\cdot\frac{\partial \boldsymbol{U}_A}{\partial s} \qquad \text{eq.3b}$$

$$\dot{\sigma} = c_\sigma = \frac{\partial\sigma}{\partial d}\left(\frac{\partial d}{\partial t} + \boldsymbol{U}_A\cdot\nabla_X d\right) - c_g\boldsymbol{k}\frac{\partial \boldsymbol{U}_A}{\partial s} \qquad \text{eq.3c}$$

which close the adiabatic part of the WAE. The right hand side of the WAE describes the physics of growth ($S_{in}$), decay ($S_{ds}$) and resonant non-linear interactions ($S_{nl4}$) among the different random waves within the discrete wave spectra as well as the near-resonant interactions ($S_{nl3}$) and the dissipative processes in shallow waters such as bottom friction ($S_{bf}$) and wave breaking ($S_{ds}$).

$$\frac{dN}{dt} = S_{total} = S_{in} + S_{nl4} + S_{ds} + S_{nl3} + S_{br} + S_{bf} \qquad \text{eq.4}$$

The most important constituents for the coupling of waves to the atmosphere are the wind input term $S_{in}$, the white-capping dissipation $S_{ds}$, and the resonant non-linear interactions in deep water. These source functions govern the distribution of wave action within the discrete wave spectra and in so doing the apparent roughness of the ocean surface, which is the clearly defined interface between the ocean and the atmosphere. At the present stage of our long term plan we focus on the effect of the surface roughness defined by the ocean waves and we neglect the thermodynamic part of the atmospheric model that of course also depends on the sea state. Further dependence on the ocean circulation and the thermodynamic balance of the ocean will be redefined in the next phase of our plan. There we will consider the influence of the waves on the ocean circulation, the fluxes of water vapour, the influence of spray formation from the ocean surface towards the atmosphere, and the generation of turbulence in the oceanic surface layer by the breaking of waves.

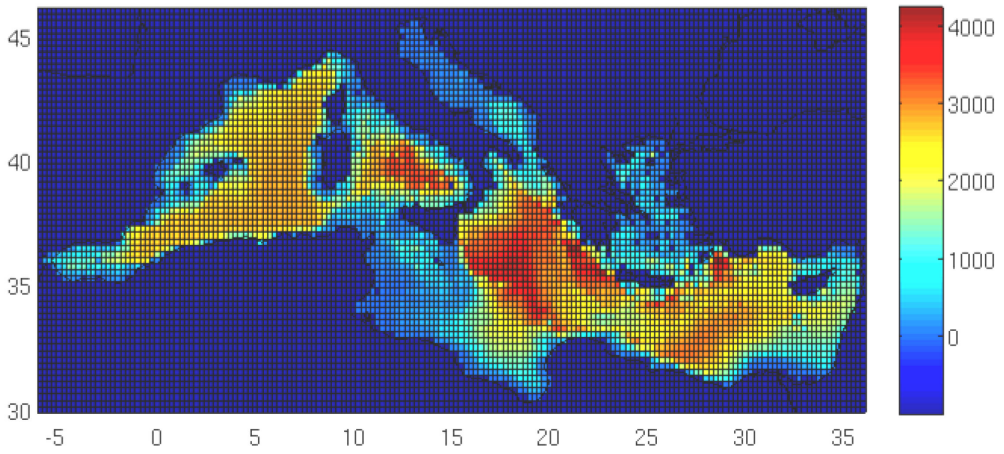


*Figure 2: Grid of the WAM model with the bathymetry of the Mediterranean Sea.*

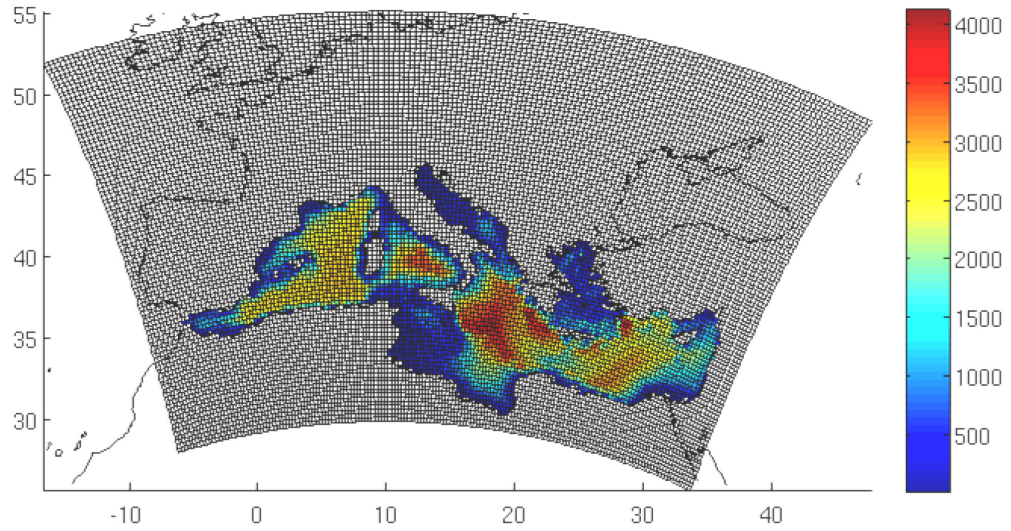


*Figure 3: Bathymetry of the Mediterranean Sea interpolated from the WAM grid on the COSMO grid using the PGMCL coupling library.*

## 2.2. The COSMO model

The COSMO model solves the non-hydrostatic, fully compressible hydro-thermodynamical equations in advection form (Eq. 1a-1d).

$$\rho \frac{d\,\mathbf{v}}{dt} = -\nabla p + \rho\,\mathbf{g} - 2\Omega \times (\rho\,\mathbf{v}) - \nabla \cdot \underline{\mathbf{t}} \qquad \text{eq.5a}$$

$$\frac{d\rho}{dt} = -\rho \nabla \cdot \mathbf{v} \qquad \text{eq.5b}$$

$$\rho \frac{dq^x}{dt} = -\nabla \cdot \mathbf{J}^x + I^x \qquad \text{eq.5c}$$

$$\rho \frac{de}{dt} = -p \nabla \cdot \mathbf{v} - \nabla \cdot \left(\mathbf{J}_e + \mathbf{R}\right) + \varepsilon \qquad \text{eq.5d}$$

where $x$ indicates the constituent of the mixing e.g. dry air ($d$), water vapour ($\mathbf{v}$), liquid water ($l$) and frozen state ($f$). The other variables represent vectors if they are bold, scalars in the other case. The involved variables are defined as follows:

| | |
|---|---|
| $t$ | time |
| $p$ | pressure |
| $T$ | temperature |
| $\rho^x$ | partial density of mixture constituent $x$ |
| $\rho = \sum_x \rho^x$ | total density of the air mixture |
| $q^x = \rho^x / \rho$ | mass fraction (specific content) of constituent $x$ |
| $v = \rho^{-1}$ | specific volume |
| $e$ | specific internal energy |
| $h = e + pv$ | specific enthalpy |
| $\mathbf{v}$ | barycentric velocity (relative to the rotating earth) |
| $I^x$ | sources/sinks of constituent $x$ |
| $\mathbf{J}^x$ | diffusion flux of constituent $x$ |
| $\mathbf{J}_e$ | diffusion flux of internal energy (heat flux) |
| $\mathbf{R}$ | flux density of solar and thermal radiation |
| $\underline{\mathbf{t}}$ | stress tensor due to viscosity |
| $\varepsilon = -\underline{\mathbf{t}} \cdot \cdot \nabla \mathbf{v}$ | kinetic energy dissipation due to viscosity |
| $\mathbf{\Omega}$ | constant angular velocity of earth rotation |
| $\mathbf{g}$ | apparent acceleration of gravity |
| $d/dt = \partial/\partial t + \mathbf{v} \cdot \nabla$ | total (Lagrangian) time derivative operator |
| $\partial/\partial t$ | local (Eulerian) time derivative operator |
| $\nabla$ | gradient (Nabla) operator |

The prognostic variables are the horizontal and vertical Cartesian wind components, temperature ($t$), pressure perturbation ($p'$, deviation from the reference state), specific humidity ($q_v$) and specific cloud water content ($q_c$); optionally: cloud ice content ($q_i$), specific water content of rain ($q_r$), snow ($q_s$) and graupel ($q_g$), the turbulent kinetic energy (tke). From these results several diagnostic variables are computed, which include the 2 metre temperature, the 10 metre wind speed, the maximum wind gusts at 10 metre height, the precipitation fluxes of rain and snow and others.

COSMO uses a rotated geographical (lat/lon) coordinate system horizontally and a generalized terrain-following height-coordinate with user defined grid stretching in the vertical. The numerical grid is based on an Arakawa C-grid, Lorenz vertical grid staggering and it uses second-order finite differences for the spatial discretization, offering also options for up to 6th order horizontal discretization, where the default is a 5th order horizontal discretization. The default time integration scheme is the 2nd and 3rd order Runge-Kutta integrator according to (Wicker and Skamarock, 2002), but also a TVD 3rd order variant of it, where there are also some other possibilities available. Numerical smoothing may be applied using 4th-order linear horizontal diffusion with option for a monotonic version including an orographic limiter, where also other options are available.

## 3. The atmospheric boundary layer and the quasi-linear theory of wind-wave interactions

The interaction of the atmosphere with the ocean surface is a fascinating and fast evolving field of physical oceanography and meteorology. Following the pioneering work of Phillips (1957) and Miles (1957), the quasi-linear theory of wave-atmosphere interactions, introduced by Peter Janssen (1989, 1991), is the one that is presently used in most of the operational wave forecasting systems worldwide. The basic assumption of Janssen's theory is that even for a young wind-sea the assumption of a logarithmic velocity profile in the atmospheric boundary layer is appropriate. Observational evidence over ocean conditions (Hristov et al., 2003), but also during strongly forced growth conditions (Troitskaya et al., 2012), underline the validity of the quasi-linear assumption made in Janssen's theory.

The formulation of the wind input source terms is:

$$S_{(\sigma,\theta),in} = \gamma \cdot N_{(\sigma,\theta)} \qquad \text{eq.6}$$

where

$$\gamma = \omega\varepsilon\beta x^2 \qquad \text{eq.7}$$

with

$$x = \left(\frac{u_*}{c}\right)\cos\left(\theta - \phi\right) \qquad \text{eq.8}$$

$$\beta = \frac{\beta_m}{\kappa^2}\mu\ln^4\left(\mu\right), \mu \le 1 \qquad \text{eq.9}$$

$$\mu = \left(\frac{u_*}{\kappa c}\right)\Omega_m e^{\frac{\kappa}{x}} \qquad \text{eq.10}$$

and $$\Omega_m = \frac{gz_0}{u_*^2} \qquad \text{eq.11}$$

Here $\mathbf{u}_*$ is the friction velocity, **c** the phase velocity, **Φ** the wind direction at 10m height and Θ the discrete wave direction of the considered wave packet. $\mathbf{\Omega_m}$ illustrates that the growth rate depends on the roughness, which inherently depends on the sea state and this justifies the tight coupling between the surface wave model and the atmosphere. $\mathbf{\Omega_m}$ (eq.11) is defined as the Charnock coefficient divided by the friction velocity. The formulation is closed by defining the kinematic stress (total stress) according to Janssen (1991) as

$$\tau = \left[ \frac{\kappa U_{(z_{obs})}}{\ln\left(\frac{z_{obs}}{z_0}\right)} \right]^2 \qquad \text{eq.12}$$

where the apparent roughness length is defined as

$$z_0 = \left( \frac{\hat{\alpha}\tau}{g\sqrt{1-\frac{\tau_w}{\tau}}} \right) \qquad \text{eq.13}$$

with the wave-induced stress given by

$$\tau_w = \varepsilon^{-1} g \int_0^{2\pi} \int_0^{\infty} \gamma N_{(\sigma,\theta)} k d\omega d\theta \qquad \text{eq.14}$$

It is important to note that beyond the discrete integration range, the prognostic part of the spectral wave model, a diagnostic $\sigma^{-5}$ tail is assumed in order to account for the high frequency contribution to the wave induced stress that cannot be neglected.

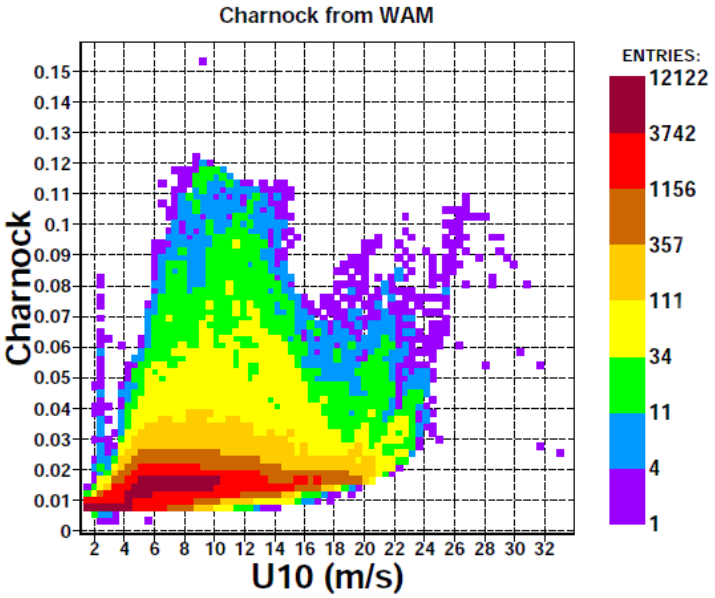


*Figure 4: Charnock coefficient computed using the coupled IFS-WAM model at the ECMWF for a two day global forecast (courtesy Jean Bidlot, ECMWF).*

The dissipation function must carefully balance the wind-input, especially in the high frequency part of the wave spectra, in order that the kinematic stress of well-known measurements (e.g. HEXOS, Katsaros et al., 1987) can be reproduced. It was found that the originally proposed formulation of Hasselmann (1974) needs to be modified in order to have realistic friction velocity estimates. Especially the high frequency part of the wave spectra was shown to be crucial in order to achieve this. For details about this consult Komen et al. (1994) and for the latest parameterization of these source terms see Bidlot et al. (2005).

# 4. The Parallel Geophysical Model Coupling Library (PGMCL) – technical part of the coupling

The coupling between the WAM and the COSMO models has been suitably done to minimize the changes in both the models and in such a way that after the compilation only one executable is present. The compilation has been totally overhauled for both codes and scripts have been used to setup automatically the dependency lists and makefiles in the proper order. In this way the final code can be compiled in parallel, e.g. by invoking the "make –j XX" command, where XX indicates the number of threads to be used during the compilation.

The code merging strategy we have developed can be applied to all the numerical source codes that are parallelized based on the MPI interface, which is the dominant parallelization framework in geophysics.

The main idea is that, when the merged program is run, the common MPI communicator is split in several MPI communicators. In practice, having N processors at disposal, we decompose them as:

$$\mathbf{N}_{ocn} + \mathbf{N}_{wav} + \mathbf{N}_{atm} = \mathbf{N}$$

Computationally, this means to split the "**MPI_COMM_WORLD**" into subsets by using the "**MPI_COM_SPLIT**" command.

Hence, after that each model is using a

- OCN_COMM_WORLD,
- ATM_COMM_WORLD and
- WAV_COMM_WORLD.

The coupling is done at instantaneous times and provides instantaneous values of the fields, i.e. no averaging is done. In other words the models are fully synchronized at the time when the exchange of information between certain models is required. It cannot be over emphasized that the above framework can hold as many models as desired, the only hurdle being that the models have to be called as subroutines within the framework of the coupling.

Depending on the value of the MPI_SPLIT either the WAM model or the COSMO model is run as the main routine. Using this approach combines both the pipe approach of limited modification to the code and the approach of full integration where every model becomes a subroutine. It also provides a useful way of abstraction since every model has its own communicator, which is one of the main benefits of the newly developed PGMCL library. However it should be pointed out that this procedure has the disadvantage that the minimal number of processors must equal the number of coupled models, However, this is a very minor problem because the multi-core architecture is now very common.

In order to continue the approach of minimal changes to each of the models, the grid of each model was not modified, see Figures 2 and 3 respectively. It is important to remember that the requirements for a numerical grid of an atmospheric model are different from the ones of a wave model. Forcing the same grid for both the models would impose on them unnecessary requirements. On the contrary the solution is to use linear interpolation. For some variables, as e.g. wind speed and direction, this is straightforward and can be done in a relatively simple way. Much more care is required for physical variables that can show substantial differences between land and sea. Obvious examples are humidity and air temperature. In this case, because we focus on the air-sea interactions, and if acting on the land-sea border, it is convenient to select only the wet points.

For the flow of information in the other direction, i.e. from the sea to the atmosphere, for each atmospheric point close to the land-sea border, out of the corresponding WAM grid points for interpolation we consider only the wet ones adapting accordingly their weight coefficients, eventually choosing the closest sea point.

This coupling strategy is very robust in terms of getting the right values at the right point. Should a more sophisticated interpolation method, as krigging or a higher order, be required, this could easily be introduced. For vectorial quantities, as wind, a previous transformation from the COSMO grid to the standard lat-lon system is required.

Once all the interpolation weights and the partition of the nodes are defined, then each node knows:

- what every other node has in its augmented domain (the domain + the ghost points)
- what every node needs for the interpolation,
- given this information the interpolation and exchange of data are executed in a single line of code that correspond to the send and receive commands of MPI.

The above formalism is near optimal in term of speed and allows efficient communication between all the models. Note that with this configuration the communication is not a bottleneck for the coupling. What can be a bottleneck in term of speed is the relative speed of the models. Therefore it is convenient to find a proper load balancing on HPFC architectures, which can be done based on work estimates and achieved iteratively during runtime. This is computer dependent; hence the optimal solution must be defined for each specific application. During the development stage the results of the exchanged fields have been systematically checked in order to guarantee their consistency.

As already mentioned, our interest is on the Mediterranean Sea (see Figure 1). For obvious reasons the COSMO and WAM models cover different areas, COSMO being expanded on a much larger grid to provide the correct high resolution results well off the boundaries. It is clear that the described exchange of information wave-atmosphere can take place only on the Mediterranean Sea. If this is not

the case, because either on land or on the Atlantic ocean, COSMO resorts back to its standard parameterization of the surface stress.

When doing the coupling, both the models actually run in parallel and exchange data at predefined times. For the wave model this time is chosen at the end of the fractional step method after the surface stress has been recalculated. For the Cosmo model this is in the middle of the integration itself, since the values are needed for the evaluation of the apparent roughness length $z_0$. The COSMO model sends to the WAM model the wind and the air density used to compute the waves. The WAM model sends back the Charnock parameter used in COSMO for the computation of the turbulence scheme.

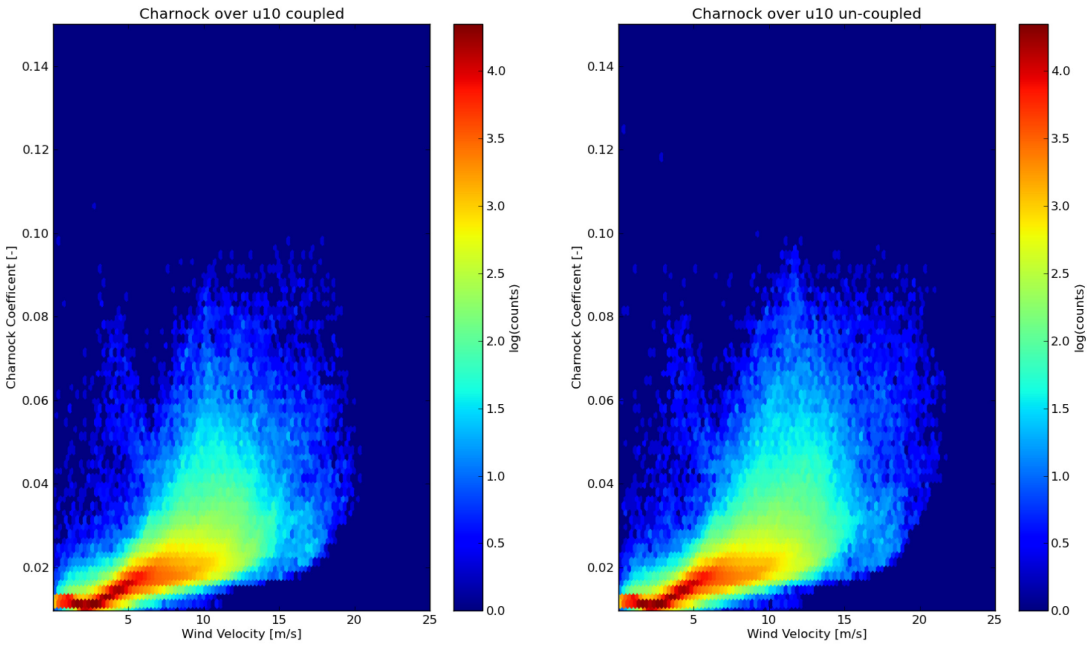


*Figure 5: Charnock coefficient for the coupled (left) and the un-coupled (right) WAM run.*

## 5. Validation of the coupled results

It is clear that a full validation of the described coupled system would require application for a long period and, most of all, coherently with operational use, a continuous data assimilation. This would allow meaningful and significant comparison with measured data. In our case, both for the used resolution (0.25°) and for not using data assimilation, we can only look for a qualitative validation. Nevertheless, because we look for the significance and implications of coupling, the results are indicative for our present purpose.

We begin with a check of the distribution of the Charnock coefficient. Figure 4 shows this distribution out of the two-day forecast of ECMWF. This is compared with the ones in Figure 5 (apologies for the different graphical system) showing the resulting distributions for the test period in the Mediterranean Sea, respectively with (left) and without (right) coupling. The experimental results match well, as range and distribution, the operational ones of ECMWF. Although the differences between the coupled and uncoupled runs are not very large, there are significant differences whose implications are clearer in the overall statistics.

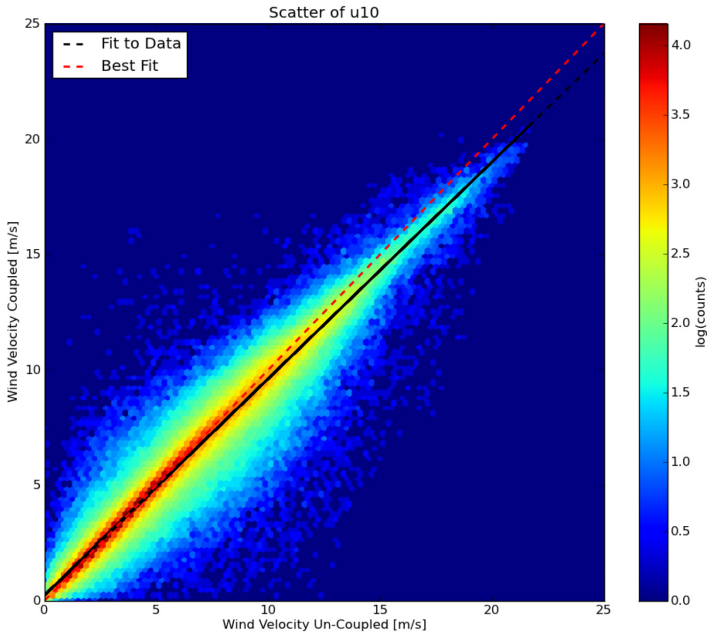


*Figure 6: Scatter plot of the wind velocities of the coupled and uncoupled model run. Line of perfect fit is red; line of best fit is black.*

The first quantitative comparison is between the corresponding (coupled vs uncoupled) 10 m wind speeds, surface atmospheric pressures and significant wave heights. Indeed, as expected, $U_{10}$ and $H_s$ are lower in the coupled runs, with also a more limited deepening of the developing low pressure systems. Figure 6 shows a comparison (scatter diagram) between the coupled and uncoupled significant wave heights. The best-fit line suggests a 5% difference between the two sets.

An interesting example is offered by the development of a cyclone in the Eastern Mediterranean during another trial period. The intense development led to an active generation, hence to a strong air-sea interaction. As expected, there are evident differences in the $H_s$, $U_{10}$ and pressure p fields (see Figure 7). While the positive and negative differences in the middle panel indicate also a shift in the position of the minimum, the obvious negative differences (coupled minus uncoupled) of significant wave heights (lowest panel) point to the clear effect of a higher surface roughness in the actively generating area.

Finally we have done an extensive comparison of the wind and wave model results versus the altimeter (Envisat, Jason and Jason-2), scatterometer (ASCAT) and buoy measured data. An example is provided in Figure 8. More in general, in Tables 1, 2 and 3 we report the overall statistics concerning $H_s$ and $U_{10}$ as derived from altimeter comparison Each table, divided into different panels, reports a) the overall (two months, Nov-Dec 2010) results for significant wave height for the couple and uncoupled runs (the parameters are defined in the Appendix), b) similar results for the wind speed, c) wave and wind essential statistics for the coupled case, and d) for the uncoupled one. The last two statistics, c) and d), are provided for single ten-day periods. There is an apparent progressive deterioration of the results (bias, RMSE) with time, that reflects the shift towards the winter and more stormy season.

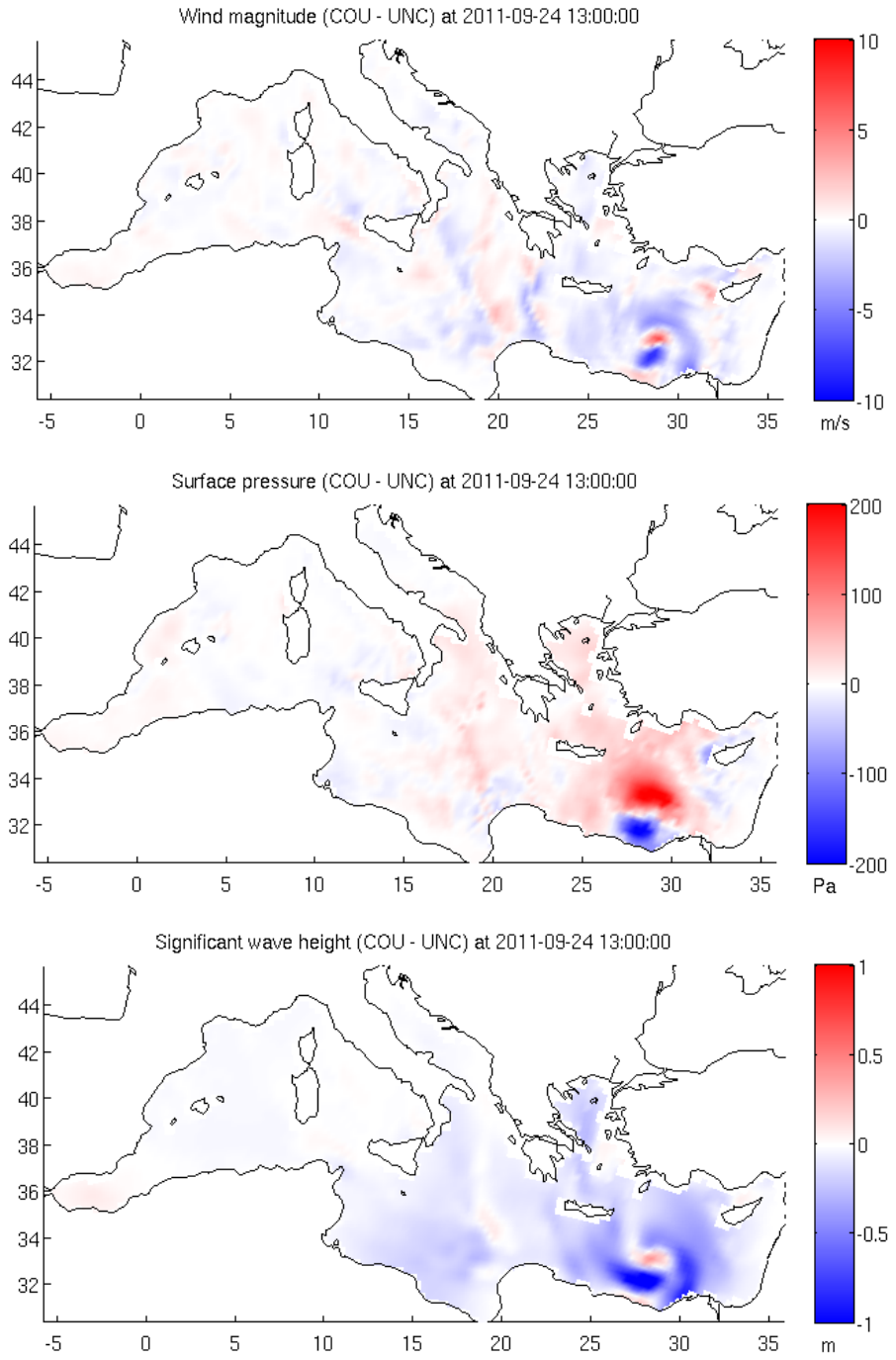


*Figure 7: Difference in wind velocity [m/s], surface pressure [Pa] and significant wave height [m] during a cyclone in the Aegean Sea at the 24.9.2011 13:00.*

The last decade of the year is a notable exception with a calm period, hence lower dimensional errors.

For our immediate interests, i.e. of comparing the coupled vs. the uncoupled runs, there is a clear, almost uniformly distributed, tendency for lower differences and parameter values in the coupled case. In particular the bias, out of an average 1.65 m $H_s$ altimeter value, is reduced of almost 50% and the scatter index of 20%. The corresponding values for $U_{10}$ are 48% and 5%.

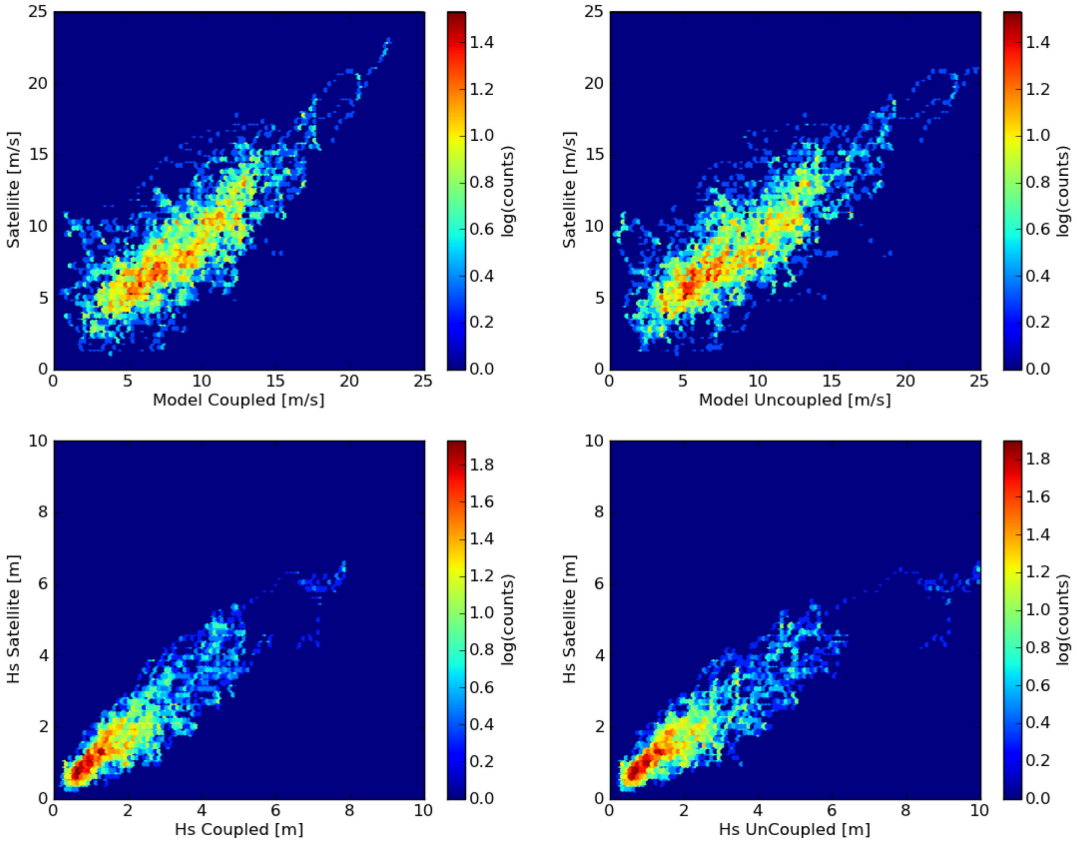


*Figure 8: Comparison of model winds and waves vs. the Jason-1 data, for the coupled and uncoupled cases.*

The same message is derived from the $U_{10}$ comparison with the ASCAT data (Table 4) and the $H_s$ versus the buoys (Table 5). In the latter, in the coupled case there is a drastic reduction of the mean error, but with still a high scatter index. We interpret this as, at least partly, associated to the coarse resolution of the wave model grid, 0.25 degree. As most of the buoys are close to the coast, this may have a remarkable influence, especially in the cases when the wind is not fully blowing from the sea towards the land.

## 6. Discussion

The COSMO and the WAM model have been coupled using an innovative coupling procedure, especially designed to allow for the different structure of the two models and the decomposition of each numerical framework. The structure of the coupling is absolutely general, capable to accommodate other models in the overall coupling procedure. The general character of the approach limits the work required for the coupling (our procedure has just 3000 lines of code). However, care is required in when, during the numerical integration of each model, the information is to be transferred between the models. As an example, during our first trials, we found unrealistic large values of the Charnock coefficient, especially close to the land-sea border. This turned out to be due to passing the reciprocal information at the wrong time combined with an error in the interpolation areas across the land-sea border.

| | | ME | AE | RMSE | CRMSE | Corr | sci | sciR |
|---|---|---|---|---|---|---|---|---|
| **Waves** | Coup | 0.25 | 0.46 | 0.65 | 0.6 | 0.88 | 0.34 | 0.32 |
| | Uncoup | 0.43 | 0.57 | 0.85 | 0.73 | 0.88 | 0.45 | 0.39 |

| | | ME | AE | RMSE | CRMSE | Corr | sci | sciR |
|---|---|---|---|---|---|---|---|---|
| **Wind** | Coup | 0.25 | 1.71 | 2.28 | 2.26 | 0.81 | 0.26 | 0.25 |
| | Uncoup | 0.44 | 1.87 | 2.44 | 2.4 | 0.81 | 0.27 | 0.27 |

| | Wave | | | Wind | | | |
|---|---|---|---|---|---|---|---|
| Period | **ME** | **AE** | **RMSE** | **ME** | **AE** | **RMSE** | |
| 11/11/2010 | -0.11 | 0.26 | 0.35 | -0.39 | 1.14 | 1.59 | NbPt=820 |
| 11/21/2010 | 0.14 | 0.28 | 0.38 | 0.12 | 1.51 | 2.04 | NbPt=636 |
| 12/1/2010 | 0.13 | 0.33 | 0.46 | 0.11 | 1.88 | 2.5 | NbPt=927 |
| 12/11/2010 | 0.19 | 0.46 | 0.63 | 0.14 | 1.58 | 2.05 | NbPt=995 |
| 12/21/2010 | 0.62 | 0.82 | 1.02 | 0.83 | 2.01 | 2.69 | NbPt=1220 |
| 12/31/2010 | 0.33 | 0.41 | 0.54 | 0.42 | 1.94 | 2.36 | NbPt=945 |

| | Wave | | | Wind | | |
|---|---|---|---|---|---|---|
| Period | **ME** | **AE** | **RMSE** | **ME** | **AE** | **RMSE** |
| 11/11/2010 | 0.02 | 0.25 | 0.39 | -0.25 | 1.22 | 1.61 |
| 11/21/2010 | 0.25 | 0.37 | 0.52 | 0.3 | 1.68 | 2.34 |
| 12/1/2010 | 0.23 | 0.38 | 0.54 | 0.27 | 1.97 | 2.64 |
| 12/11/2010 | 0.36 | 0.52 | 0.77 | 0.38 | 1.57 | 2.05 |
| 12/21/2010 | 0.98 | 1.09 | 1.36 | 1.25 | 2.43 | 3.04 |
| 12/31/2010 | 0.45 | 0.53 | 0.77 | 0.32 | 2.06 | 2.43 |

*Table 1: Comparison of wind and wave model results versus the Envisat altimeter data. The results are provided for significant wave height (m) and wind speed (m/s). See the Appendix for the meaning of the statistical parameters. The two larger panels show the statistics for each ten day period (end day indicated).*

| | | ME | AE | RMSE | CRMSE | Corr | sci | sciR |
|---|---|---|---|---|---|---|---|---|
| **Waves** | Coup | 0.13 | 0.39 | 0.54 | 0.52 | 0.90 | 0.31 | 0.30 |
| | Uncoup | 0.29 | 0.47 | 0.71 | 0.65 | 0.90 | 0.42 | 0.38 |

| | | ME | AE | RMSE | CRMSE | Corr | sci | sciR |
|---|---|---|---|---|---|---|---|---|
| **Wind** | Coup | 0.09 | 1.59 | 2.12 | 2.12 | 0.81 | 0.25 | 0.25 |
| | Uncoup | 0.23 | 1.71 | 2.25 | 2.24 | 0.82 | 0.27 | 0.26 |

| | Wave | | | Wind | | | |
|---|---|---|---|---|---|---|---|
| Period | **ME** | **AE** | **RMSE** | **ME** | **AE** | **RMSE** | |
| 11/11/2010 | -0.16 | 0.27 | 0.31 | -0.33 | 1.03 | 1.30 | NbPt=1119 |
| 11/21/2010 | -0.01 | 0.20 | 0.27 | -0.29 | 1.43 | 1.86 | NbPt=1291 |
| 12/1/2010 | 0.04 | 0.28 | 0.37 | 0.19 | 1.33 | 1.72 | NbPt=1402 |
| 12/11/2010 | 0.03 | 0.31 | 0.42 | -0.07 | 1.23 | 1.70 | NbPt=1453 |
| 12/21/2010 | 0.24 | 0.53 | 0.67 | -0.39 | 2.27 | 2.95 | NbPt=1480 |
| 12/31/2010 | 0.65 | 0.74 | 0.89 | 1.53 | 2.18 | 2.61 | NbPt=1248 |

| | Wave | | | Wind | | |
|---|---|---|---|---|---|---|
| Period | **ME** | **AE** | **RMSE** | **ME** | **AE** | **RMSE** |
| 11/11/2010 | -0.01 | 0.26 | 0.33 | -0.08 | 1.03 | 1.32 |
| 11/21/2010 | 0.07 | 0.23 | 0.34 | -0.24 | 1.36 | 1.77 |
| 12/1/2010 | 0.10 | 0.28 | 0.38 | 0.24 | 1.35 | 1.73 |
| 12/11/2010 | 0.16 | 0.37 | 0.55 | 0.02 | 1.43 | 1.91 |
| 12/21/2010 | 0.51 | 0.70 | 0.90 | -0.25 | 2.49 | 3.13 |
| 12/31/2010 | 0.90 | 0.97 | 1.26 | 1.77 | 2.47 | 2.89 |

*Table 2: As Table 1, but for Jason altimeter.*

| | | ME | AE | RMSE | CRMSE | Corr | sci | sciR |
|---|---|---|---|---|---|---|---|---|
| **Waves** | Coup | 0.11 | 0.37 | 0.5 | 0.49 | 0.88 | 0.31 | 0.3 |
| | Uncoup | 0.24 | 0.43 | 0.58 | 0.53 | 0.88 | 0.36 | 0.32 |

| | | ME | AE | RMSE | CRMSE | Corr | sci | sciR |
|---|---|---|---|---|---|---|---|---|
| **Wind** | Coup | 0.17 | 1.57 | 2.08 | 2.08 | 0.82 | 0.27 | 0.27 |
| | Uncoup | 0.32 | 1.63 | 2.13 | 2.11 | 0.82 | 0.28 | 0.27 |

| | Wave | | | Wind | | | |
|---|---|---|---|---|---|---|---|
| Period | ME | AE | RMSE | ME | AE | RMSE | |
| 11/11/2010 | -0.24 | 0.29 | 0.39 | -0.35 | 1.18 | 1.52 | NbPt=1449 |
| 11/21/2010 | -0.05 | 0.22 | 0.28 | 0.14 | 1.3 | 1.67 | NbPt=1268 |
| 12/1/2010 | 0.14 | 0.31 | 0.4 | 0.08 | 1.47 | 1.86 | NbPt=1689 |
| 12/11/2010 | 0.08 | 0.28 | 0.39 | 0.28 | 1.33 | 1.73 | NbPt=1500 |
| 12/21/2010 | 0.24 | 0.41 | 0.52 | -0.18 | 2.22 | 2.84 | NbPt=1668 |
| 12/31/2010 | 0.33 | 0.45 | 0.61 | 1.04 | 1.79 | 2.41 | NbPt=1540 |

| | Wave | | | Wind | | |
|---|---|---|---|---|---|---|
| Period | ME | AE | RMSE | ME | AE | RMSE |
| 11/11/2010 | -0.14 | 0.28 | 0.37 | -0.26 | 1.24 | 1.58 |
| 11/21/2010 | 0.01 | 0.22 | 0.28 | 0.18 | 1.33 | 1.71 |
| 12/1/2010 | 0.25 | 0.37 | 0.49 | 0.21 | 1.51 | 1.93 |
| 12/11/2010 | 0.13 | 0.31 | 0.42 | 0.3 | 1.42 | 1.83 |
| 12/21/2010 | 0.41 | 0.51 | 0.66 | 0.26 | 2.19 | 2.72 |
| 12/31/2010 | 0.47 | 0.52 | 0.74 | 1.19 | 1.99 | 2.62 |

*Table 3: As Table 1, but for Jason-2 altimeter.*

| | | | |
|---|---|---|---|
| Coup | ME=0.61 | AE=1.93 | RMSE=2.56 |
| Uncoup | ME=0.77 | AE=2.04 | RMSE=2.69 |

*Table 4: Comparison between the coupled and uncoupled COSMO wind speeds (m/s) vs the ASCAT data. See the Appendix for the meaning of the statistical parameters.*

| | ME | AE | RMSE | CRMSE | Corr | sci | sciR |
|---|---|---|---|---|---|---|---|
| **Coup** | 0.11 | 0.39 | 0.55 | 0.54 | 0.77 | 0.42 | 0.42 |
| **Uncoup** | 0.21 | 0.43 | 0.62 | 0.58 | 0.77 | 0.48 | 0.45 |

*Table 5: Comparison between the coupled and uncoupled WAM significant wave heights (m) versus all the buoys present in the Mediterranean Sea. See the Appendix for the meaning of the statistical parameters.*

The models have been tested and shown to be stable and robust. Their validation has shown that the most important parameters are in the expected range. Also the qualitative validation of the coupled model is giving the anticipated effect on the atmospheric boundary layer as well as for the surface wave model. For a young and growing wind sea the effect of the coupling of COSMO to WAM results in an increased apparent roughness length coming along with reduced wind velocities that are compensated with increased pressure, which reduces the pressure gradients in cyclonic wind fields as it is anticipated.

Although their significance is partly limited by running the experiments without data assimilation (the system is driven only by the boundary conditions), the extended comparison with multiple altimeter significant wave heights and wind speeds strongly suggests that the coupling leads to a substantial reduction of errors.

In the next phase of this project we plan 1) after the necessary further tests, to make operational the present system at the Italian Meteorological Service CNMCA, where presently WAM is run as a slave of COSMO, 2) to add to the coupling also the ROMS circulation model, so as to have fully coupled atmosphere and ocean in the Mediterranean Sea.

## References

Ardhuin, F.,Jenkins, A.D., 2006: On the Interaction of Surface Waves and Upper Ocean Turbulence. J. Phys. Oceanogr., 36, 551–557. doi: http://dx.doi.org/10.1175/JPO2862.1

Bidlot, J., S. Abdalla, and P. Janssen, 2005: A revised formulation for ocean wave dissipation in CY25R1. Tech. Rep. Memorandum R60.9/JB/0516, Research Department,

Babanin, A.V., 2006: On a wave-induced turbulence and a wave-mixed upper ocean layer. Geophysical Research Letters, 33, L20605, doi:10.1029/2006GL027308, 6p

Bretherton, F.P. and Garrett, C.J.R., 1969. Wave trains in inhomogeneous moving media. Proc. Roy. Soc., A302, 529-554.

Cavaleri, L., B. Fox-Kemper, M.Hemer, 2012, Wind waves in the coupled climate system, *Bull. Amer. Meterol. Soc*., to be published

Charnock, H., 1955. Wind stress on a water surface. Q. J. Royal Meteorol. Soc. 81, 639-640.

ECMWF, 2012, IFS documentation, http://www.ecmwf.int/research/ifsdocs/

Hasselmann, K., 1961. On the non-linear energy transfer in a gravity-wave spectrum. Part 1. General theory. J. Fluid Mech., 12, 481–500.

Hasselmann, K., 1974. On the spectral dissipation of ocean waves due to whitecapping. Bound.-Layer Meteor., 6, 107-127.

Hristov, T., S. Miller, C. Friehe, “Dynamical coupling of wind and ocean waves through wave-induced air flow”, Nature, v. 422, pp. 55--58, 2003.

Janssen, P.A.E.M., 1982. Quasilinear approximation for the spectrum of wind-generated water waves. J. Fluid Mech. 117, 493-506.

Janssen, P.A.E.M., 1989. Wave-induced stress and the drag of air flow over sea waves. J. Phys. Oceanogr. 19, 745-754.

Janssen, P.A.E.M., 1991. Quasi-linear theory of wind wave generation applied to wave forecasting. J. Phys. Oceanogr. 21, 1631-1642.

Janssen, P. A. E. M., O. Saetra, C. Wettre, H. Hersbach , 2004, Impact of the sea state on the atmosphere and ocean, Annales Hydrographiques, Vol. 6e série, vol. 3, No. 772. (2004)

Janssen. P.A.E.M. 2010, Ocean wave effects on the daily cycle in STT, ECMWF, Technical Memorandum.

Keller, J.B., 1958. Surface waves on water on non-uniform depth. Journal of Fluid Mechanics 4, 607–614.

Katsaros, K.B., S.D. Smith and W.A. Oost, 1987. HEXOS - Humidity Exchange Over the Sea. A program for research on water-vapor and droplet fluxes from sea to air at moderate to high wind speeds. Bull. Amer. Meteor. Soc. 68, 466-476.

Komen, G.J., L. Cavaleri, M. Donelan, K. Hasselmann, S. Hasselmann, and P.A.E.M. Janssen, 1994. Dynamics and Modelling of Ocean Waves, Cambridge University Press, Cambridge.

Makin, V.K.: 2005, 'A note on drag of the sea surface at hurricane winds', Boundary-Layer Meteorol.,115, 169-176.

Miles, J.W., 1957. On the generation of surface waves by shear flows. J. Fluid Mech. 3, 185-204.

Phillips, O.M., 1957. On the generation of surface waves by turbulent wind. J. Fluid Mech., 2, 417-445.

Troitskaya, Y. I., O. Druzhinin, and S. Zilitinkevich (2012), Direct numerical simulation of a turbulent wind over a wavy water surface, J. Geophys. Res., doi:10.1029/2011JC007789, in press.

WAMDI group: S. Hasselmann, K. Hasselmann, E. Bauer, P.A.E.M. Janssen, G.J. Komen, L. Bertotti, P. Lionello, A. Guillaume, V.C. Cardone, J.A. Greenwood, M. Reistad, L. Zambresky and J.A. Ewing, 1988. The WAM model - a third generation ocean wave prediction model. J. Phys. Oceanogr. 18, 1775-1810.

## Acknowledgements

We are indebted to Jean Bidlot and Peter Janssen for the extensive information concerning the system operational at the European Centre for Medium-Range Weather Forecasts.

## Appendix: Statistical formula

Suppose that we have N measurement $\boldsymbol{x}'_i$ and corresponding N modelled values $\boldsymbol{x}_i$. Then the mean error of the model, or bias, is defined as

$$ME = \frac{1}{N}\sum_{i=1}^{N} x'_i - x_i$$

The absolute error of the model is defined as

$$AE = \frac{1}{N}\sum_{i=1}^{N} | x'_i - x_i |$$

The Root Mean Square Error of the model is defined

$$RMSE = \sqrt{\frac{1}{N}\sum \left(x'_i - x_i\right)^2}$$

The Centered Root Mean Square Error is defined as

$$CRMSE = \sqrt{RMSE^2 - ME^2}$$

The Correlation is defined as

$$Corr = \frac{\sum_{i=1}^{N} \left(x'_i - m(x')\right)\left(x_i - m(x)\right)}{\sqrt{\sum_{i=1}^{N} \left(x'_i - m(x')\right)^2 \sum_{i=1}^{N} \left(x_i - m(x)\right)^2}}$$

with

$$m(x) = \frac{1}{N}\sum_{i=1}^{N} x_i$$

The Scatter Index is defined as

$$SI = \frac{RMSE}{m(x)}$$

The Centered Scatter Index is defined as

$$CSI = \frac{CRMSE}{m(x)}$$